NASA Technical Memorandum 85713

Aerodynamic Characteristics of a Sparrow III Missile Model in the Flow Field of a Generalized Parent Body at Mach 2.86

Robert L. Stallings, Jr.

FEBRUARY 1984

NASA

NASA Technical Memorandum 85713

Aerodynamic Characteristics of a Sparrow III Missile Model in the Flow Field of a Generalized Parent Body at Mach 2.86

Robert L. Stallings, Jr.
Langley Research Center
Hampton, Virginia

NASA
National Aeronautics
and Space Administration

Scientific and Technical
Information Office

1984

INTRODUCTION

For high-speed fighters capable of supersonic weapons delivery, information concerning the effect of store separation distance on the store aerodynamic characteristics at supersonic speeds is required to insure safe store separation. Most of the existing supersonic separation data were obtained during development of specific airplane configurations and, therefore, have limited general application. The existing data are also somewhat cumbersome to model for theoretical test cases because of the complexity of the parent-body flow field. In order to provide some basic store aerodynamic data for a range of store separation distances at supersonic speeds, a test program was initiated at the NASA Langley Research Center using existing models consisting of a Sparrow III wing-control missile model (ref. 1) that represented the store and a splitter plate that represented the parent aircraft. The splitter plate was tested with and without circular-arc protuberances attached to its surface.

The tests were conducted in the low-speed test section of the Langley Unitary Plan Wind Tunnel at a Mach number of 2.86 and a Reynolds number per meter of 6.56×10^6.

SYMBOLS

C_A	axial-force coefficient, $\frac{\text{Axial force}}{qS}$
C_m	pitching-moment coefficient, $\frac{\text{Pitching moment}}{qSL}$
C_N	normal-force coefficient, $\frac{\text{Normal force}}{qS}$
D	store body diameter, 3.048 cm
h	circular-arc protuberance height, cm
L	store length, 54.86 cm
q	free-stream dynamic pressure, Pa
S	store body cross-sectional area, 7.297×10^{-4} m^2
V_∞	free-stream velocity vector, m/sec
X	surface distance downstream from plate leading edge, cm
X_p	value of X at location of protuberance leading edge, cm
X_s	value of X at location of store nose, cm
ΔX_{sp}	increment in X from protuberance trailing edge to store nose, cm

Z	perpendicular distance from plate surface to store axis of symmetry (store separation distance), cm
ϕ	store model roll angle, deg

APPARATUS AND METHODS

Wind Tunnel and Test Conditions

The tests were conducted in the Langley Unitary Plan Wind Tunnel. This facility is a variable-pressure continuous-flow wind tunnel with two test sections that permit a variation in Mach number from 1.5 to 4.6. Ahead of each test section is an asymmetric nozzle that permits a continuous variation in Mach number from 1.5 to 2.9 in the low Mach number test section and from 2.3 to 4.6 in the high Mach number test section. The test sections are approximately 2.1 m long and have a cross-sectional area of approximately 1.2 m^2. A complete description of the facility is given in reference 2.

The free-stream test conditions were a Mach number of 2.86, a free-stream Reynolds number per meter of 6.56×10^6, a stagnation pressure of 98.54 kPa, and a stagnation temperature of 339 K.

Models

The general arrangement of the store model and the splitter plate that represented the parent aircraft is shown in figure 1. Photographs of the store model and splitter plate are shown in figure 2.

The store model geometry (fig. 3) consisted of an ogive-cylinder body, cruciform wings, and in-line tails. The wings had a trapezoidal planform and a diamond airfoil section. The tails had a triangular planform and a modified diamond airfoil section. Relative to the splitter plate surface, the model was tested at zero angle of attack, zero angle of yaw, and roll angles of 0° and 45°.

The parent aircraft for the present test was represented by a vertical splitter plate that extended from the floor to the ceiling of the test section and was approximately 1.8 m in length. Photographs of the plate are shown in figure 2 and basic dimensions are given in figure 4(a). In order to establish supersonic flow on the back side of the flat plate, which was required to eliminate contamination of the front surface due to spillage, the back side discharge area was increased by inclining the plate 1° relative to the free-stream flow, as shown in figure 4(a). Because the flow over the plate is two-dimensional and the centerline of the store model is always parallel to the flat-plate surface, the major effect of this 1° angle is a small change in the local flow conditions on the plate. For example, the local Mach number of the flat-plate flow field is 2.81 rather than 2.86 and the local nominal Reynolds number per meter is 6.72×10^6 rather than 6.56×10^6. It should be noted that all force and moment data reductions were based on free-stream conditions rather than the local plate conditions.

Two-dimensional circular-arc protuberances were attached to the flat plate as shown in figure 1 to perturb the flat-plate flow field in some tests. Photographs of the flat-plate assembly with a protuberance attached at two different stations are shown in figure 2. The basic dimensions of the circular-arc protuberances are given

in figure 4(b). Protuberances with thicknesses of 1.27 and 2.54 cm were constructed and tested. Each protuberance was tested with its leading edge coincident with the flat-plate leading edge and at a location 33.02 cm downstream of the plate leading edge, as indicated in figure 1.

A boundary-layer transition strip consisting of randomly distributed No. 50 sand (0.032 cm nominal height) in a 0.159-cm-wide band was applied to the flat plate 1.02 cm downstream from the leading edge. For the store model, transition strips consisted of individually applied No. 40 sand elements (0.046 cm nominal height) spaced about 0.184 cm between centers measured perpendicular to the airstream. The strips were located on the wings and fins 1.02 cm streamwise downstream from the leading edges and on the nose 3.05 cm downstream from the apex.

Measurements

Aerodynamic forces and moments of the store were measured with a six-component strain gage balance. Since the forces and moments in the lateral plane were essentially zero because of lateral flow symmetry, only the three components of data about the longitudinal axis (C_N, C_m, and C_A) are presented. No corrections have been applied to the present data for chamber pressure. Chamber pressures were measured for part of the test conditions and were found to remain approximately constant at a value corresponding to a chamber axial-force coefficient of 0.070, which is in good agreement with results presented in reference 1.

RESULTS AND DISCUSSION

In order to facilitate discussion of the store separation data, estimates of the boundaries of the protuberance flow field were determined from the second-order inviscid approximation of Friedrich (ref. 3) and are shown in figure 5 relative to the store separation matrix for the two protuberance heights and locations. Store separation distances are shown for both the forward store station (X_s = 84.77 cm) and the aft store station (X_s = 105.09 cm).

Figure 6 shows store aerodynamic characteristics ($\phi = 0°$) for the two protuberance locations (X_p = 0 and 33.02) and the two store stations for each protuberance location. The results presented in figures 6(a) through 6(d) are for decreasing values of ΔX_{sp} ranging from the maximum separation distance of 59.37 cm to the minimum separation distance of 6.03 cm. The data presented show that for $\Delta X_{sp} \geqslant 39.05$ (figs. 6(a) and 6(b)) and $Z/D < 4$, protuberance height has only minor effects on the store separation characteristics. This trend indicates that the variation in C_m and C_N for this range of Z/D is a result of local interactions between the store model and the flat plate rather than changes in the protuberance flow field. The calculated flow boundaries for this range of Z/D and ΔX_{sp} presented in figures 5(a) and 5(b) show that the store model is located between the flat-plate surface and the protuberance trailing-edge shock. Therefore, its aerodynamic characteristics would not be expected to be significantly affected by the protuberance flow field.

The flow boundaries presented in figures 5(a) and 5(b) indicate that for the aft store station (ΔX_{sp} = 59.37) the store model penetrates the protuberance flow field at $Z/D \approx 5$ or 6, and for the more forward store station (ΔX_{sp} = 39.05), at $Z/D \approx 3.5$ or 4. Once the store model penetrates the protuberance flow field, its aerodynamic characteristics are affected by protuberance height, as shown, for

example, in figure 6(b) for $\Delta X_{sp} = 39.05$. As the nose of the store model enters the protuberance flow field, it is exposed to an upwash region created by the flow expanding over the rear half of the protuberance. This upwash region results in an increase in the store pitching moment. For $\Delta X_{sp} = 39.05$ (fig. 6(b)), the increase in C_m initially occurs at $Z/D \approx 4$, and for $h = 1.27$, a peak value is obtained at $Z/D \approx 8$.

At $Z/D \approx 8$, the nose of the model is located in the vicinity of the flow field where the local flow direction is parallel to the free-stream direction (fig. 5(a)) and the wings are just inside the trailing-edge shock. With further increases in Z/D, the model nose is located in the downwash region created by the forward half of the protuberance. Thus, a decrease in C_m results. Minimum values of C_m were obtained at $Z/D \approx 12$. For the 1.27-cm protuberance, the store normal-force coefficient for $\Delta X_{sp} = 39.05$ (fig. 6(b)) remained approximately constant at $4 < Z/D < 7$. At $Z/D \approx 7$, the store model wing crosses the trailing-edge shock, resulting in a sharp increase in C_N. Peak values are measured at $Z/D \approx 10$. Also for $\Delta X_{sp} = 39.05$, the store axial-force coefficients generally decrease with increasing Z/D at $Z/D < 5$ and increase with further increases in Z/D at $5 < Z/D < 12$. In general, the results of figure 6(b) show that at $Z/D > 4$, increasing h results in an increase in the magnitude of the maximum store pitching-moment coefficient and normal-force coefficient and a decrease in the value of Z/D at which peak pitching-moment coefficient is measured. The results presented in figure 6(b) also show that increasing h results in a slight decrease in the value of Z/D at which the model nose and the model wings cross the protuberance flow-field trailing-edge shock, as indicated by the onset of the positive gradients in C_m and C_N, respectively. Increasing h also results in a decrease in the minimum measured value of C_A.

The results presented in figures 6(a) through 6(d) show that for a given protuberance height the trends with Z/D discussed for figure 6(b) are somewhat similar for the range of ΔX_{sp} tested, although there is a shift in the aerodynamic coefficient distributions toward the plate surface with decreasing ΔX_{sp} because of the protuberance flow field approaching the plate surface. For the minimum store-protuberance separation distance, $\Delta X_{sp} = 6.03$ (fig. 6(d)), a large portion of the store model is contained within the protuberance flow field at the minimum test value of Z/D. Therefore, for this minimum store-protuberance separation distance, protuberance height has a large effect on the store aerodynamic characteristics, in contrast to the negligible effect shown previously for the maximum separation distance.

The effect of roll angle on the store model separation characteristics is shown in figure 7. In general, the results show no significant effect of roll angle for the range of test variables.

The aerodynamic characteristics of the store model with and without the store wings attached are presented in figure 8 for $\phi = 0°$. The model tails were not removed for either of these configurations. The results presented in figure 8(a) are for the clean plate carriage configuration and show that the store wings make little if any contributions to the store pitching-moment or normal-force coefficients - even for values of $Z/D < 4$ - where the store model and flat-plate flow-field interactions affect the store aerodynamic characteristics, as shown previously. The data show the anticipated reduction in C_A with removal of the wings. Presented in figure 8(b) are data for $h = 1.27$ and $\Delta X_{sp} = 26.35$. These results show that in the protuberance flow field the wings make significant contributions to both C_N and C_m. Similar trends are noted in figure 8(c) for $\Delta X_{sp} = 6.03$.

CONCLUDING REMARKS

Measurements of the longitudinal aerodynamic characteristics of a Sparrow III missile model with wing controls have been obtained through a range of separation distances relative to a flat-plate surface representing the parent-body configuration. Data were obtained both with and without two-dimensional circular-arc protuberances attached to the flat-plate surface. The tests were conducted in the low Mach number test section of the Langley Unitary Plan Wind Tunnel at a Mach number of 2.86 and a Reynolds number per meter of 6.56×10^6. The following results were obtained from these tests:

1. The behavior of the store aerodynamic characteristics with varying separation distance in the flow field created by the flat plate and protuberance was generally as would be expected on the basis of flow-field boundaries determined from the second-order approximation of Friedrich.

2. When the store model was located between the flat-plate surface and the protuberance trailing-edge shock, its aerodynamic characteristics were not affected by protuberance height, although the interactions between the store model and the flat-plate flow field created a small effect.

3. In general, varying roll angle from 0° to 45° caused no significant effect on the store separation characteristics.

Langley Research Center
National Aeronautics and Space Administration
Hampton, VA 23665
December 18, 1983

REFERENCES

1. Monta, William J.: Supersonic Aerodynamic Characteristics of a Sparrow III Type Missile Model With Wing Controls and Comparison With Existing Tail-Control Results. NASA TP-1078, 1977.

2. Jackson, Charlie M., Jr.; Corlett, William A.; and Monta, William J.: Description and Calibration of the Langley Unitary Plan Wind Tunnel. NASA TP-1905, 1981.

3. Lighthill, M. J.: Higher Approximations in Aerodynamic Theory. Princeton Univ. Press, 1960.

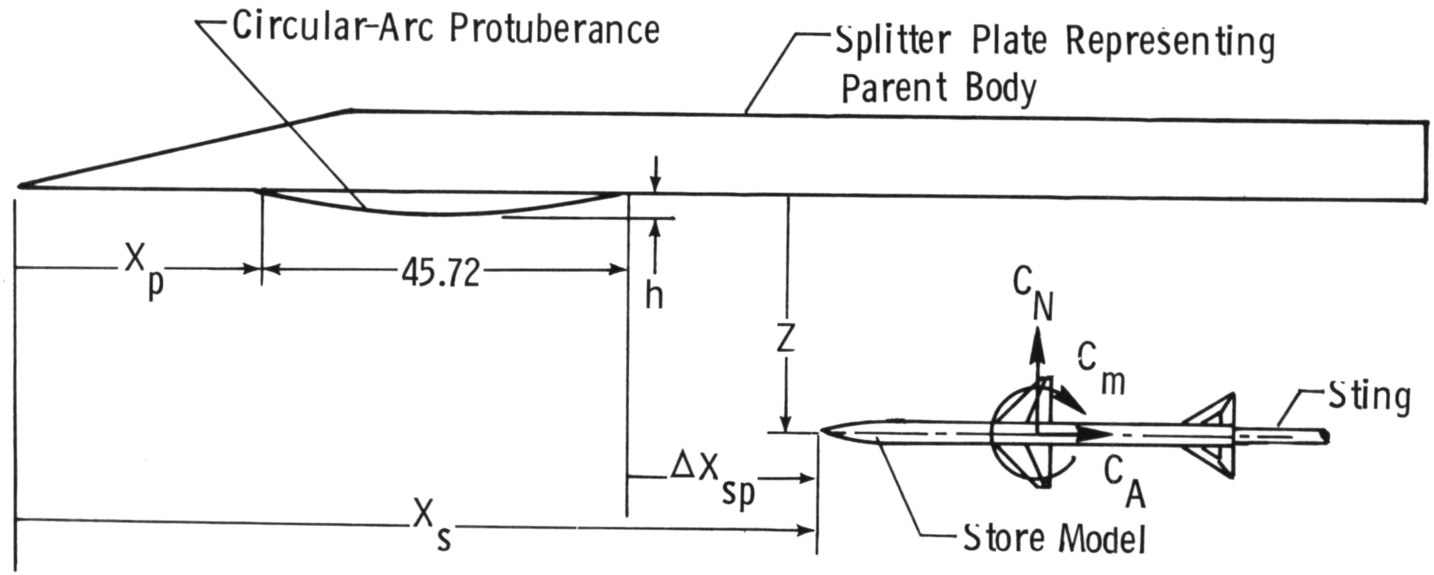

$h = 1.27,\ 2.54$

$X_p = 0,\ 33.02$

$X_s = 84.77,\ 105.09$

$\Delta X_{sp} = 6.03,\ 26.35,\ 39.05,\ 59.37$

Figure 1.- General arrangement of models. (All dimensions are in centimeters unless otherwise noted.)

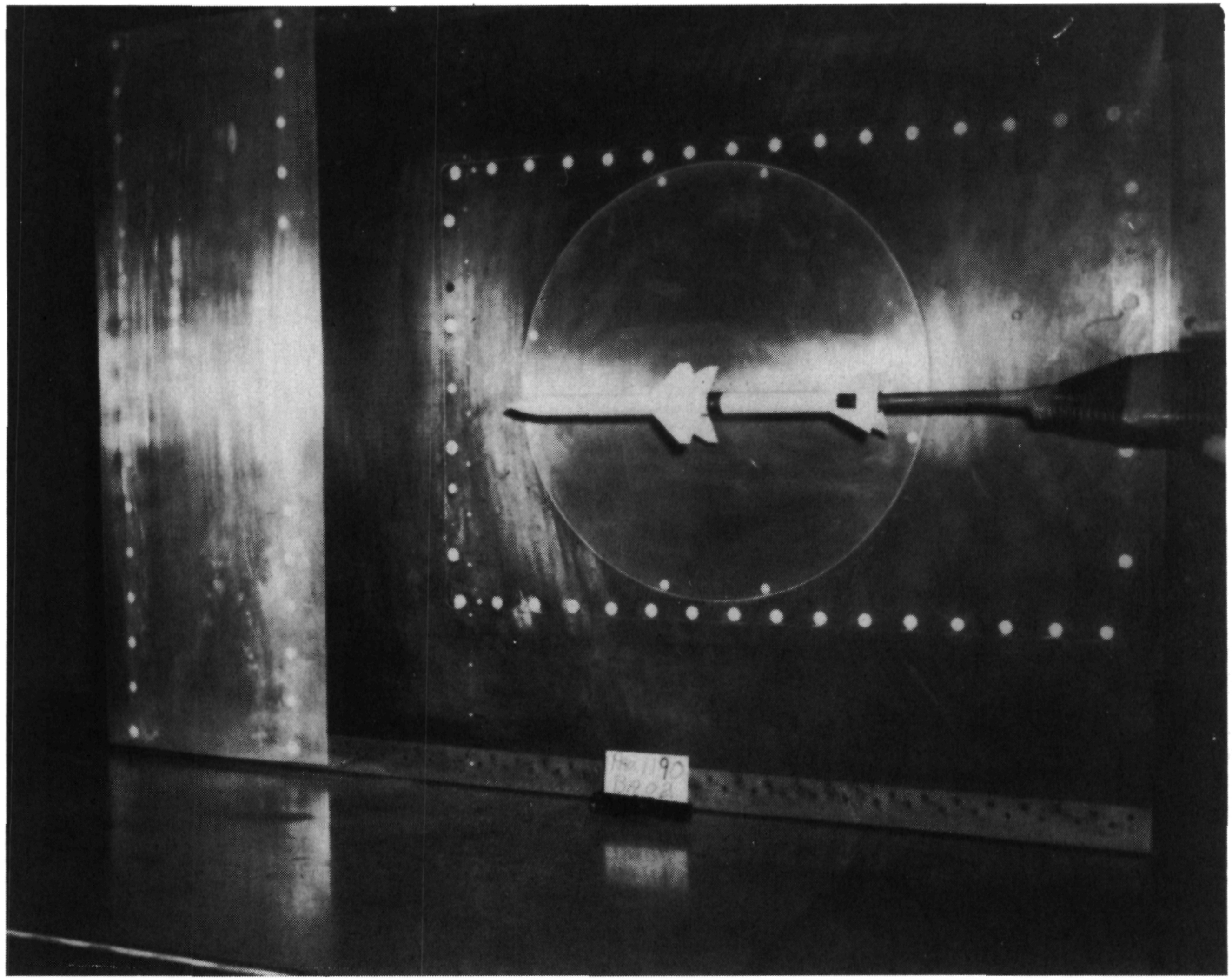

L-83-148

(a) $X_p = 0$; $h = 1.27$ cm; $\phi = 45°$.

Figure 2.- Model installation photographs.

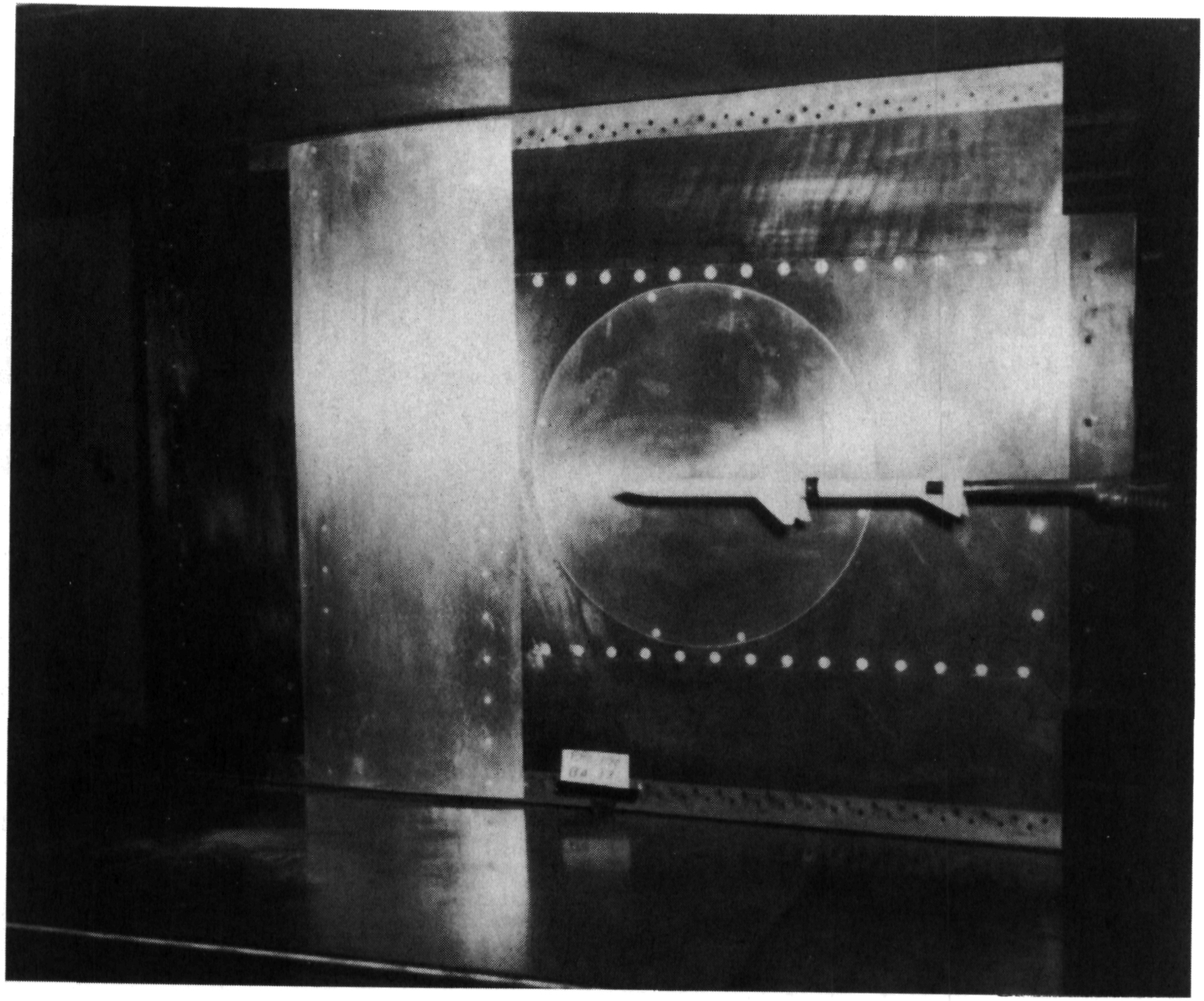

L-83-149

(b) $X_p = 33.02$ cm; $h = 2.54$ cm; $\phi = 45°$.

Figure 2.- Concluded.

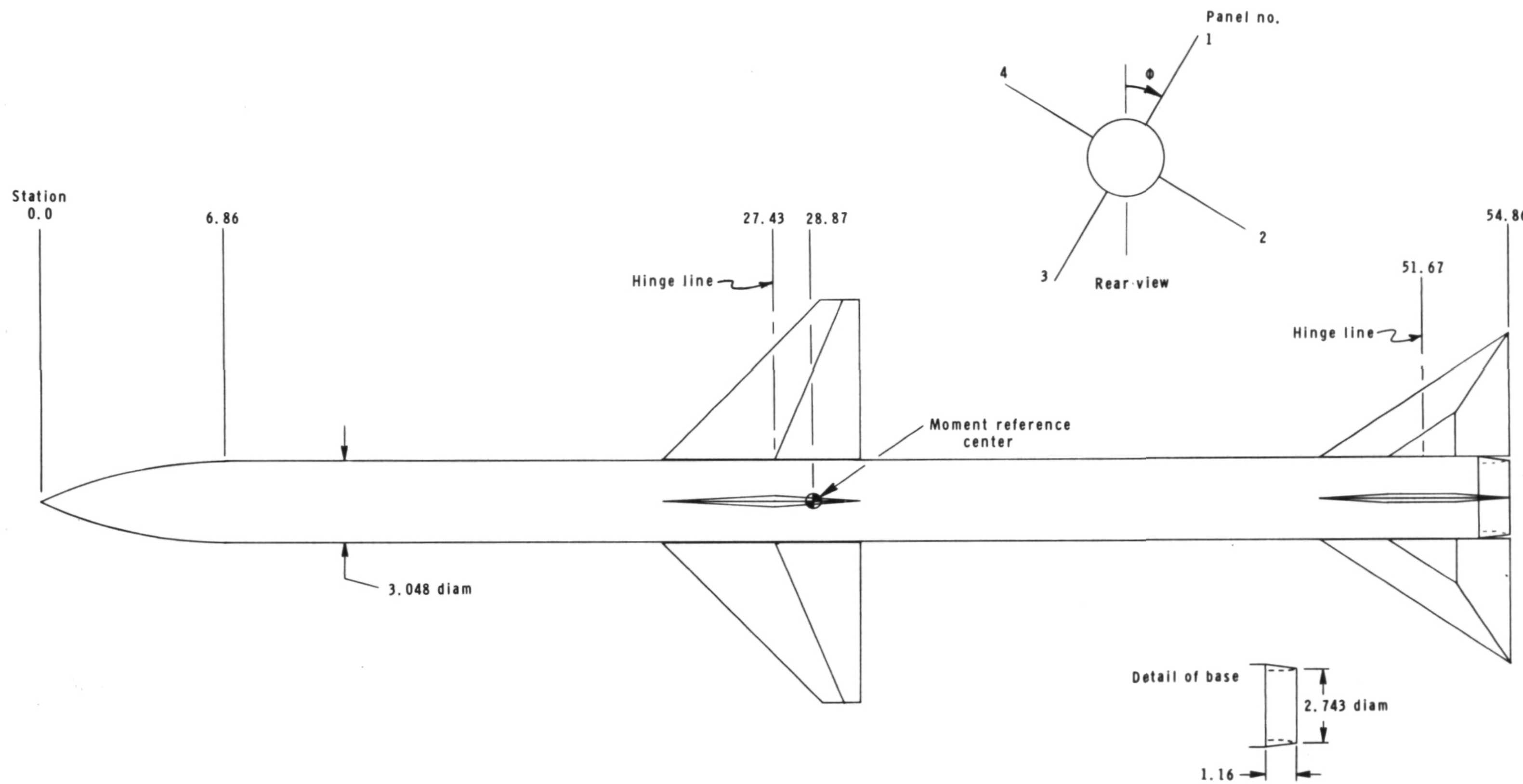

(a) Complete model.

Figure 3.- Store model drawings. (All dimensions are in centimeters unless otherwise noted.)

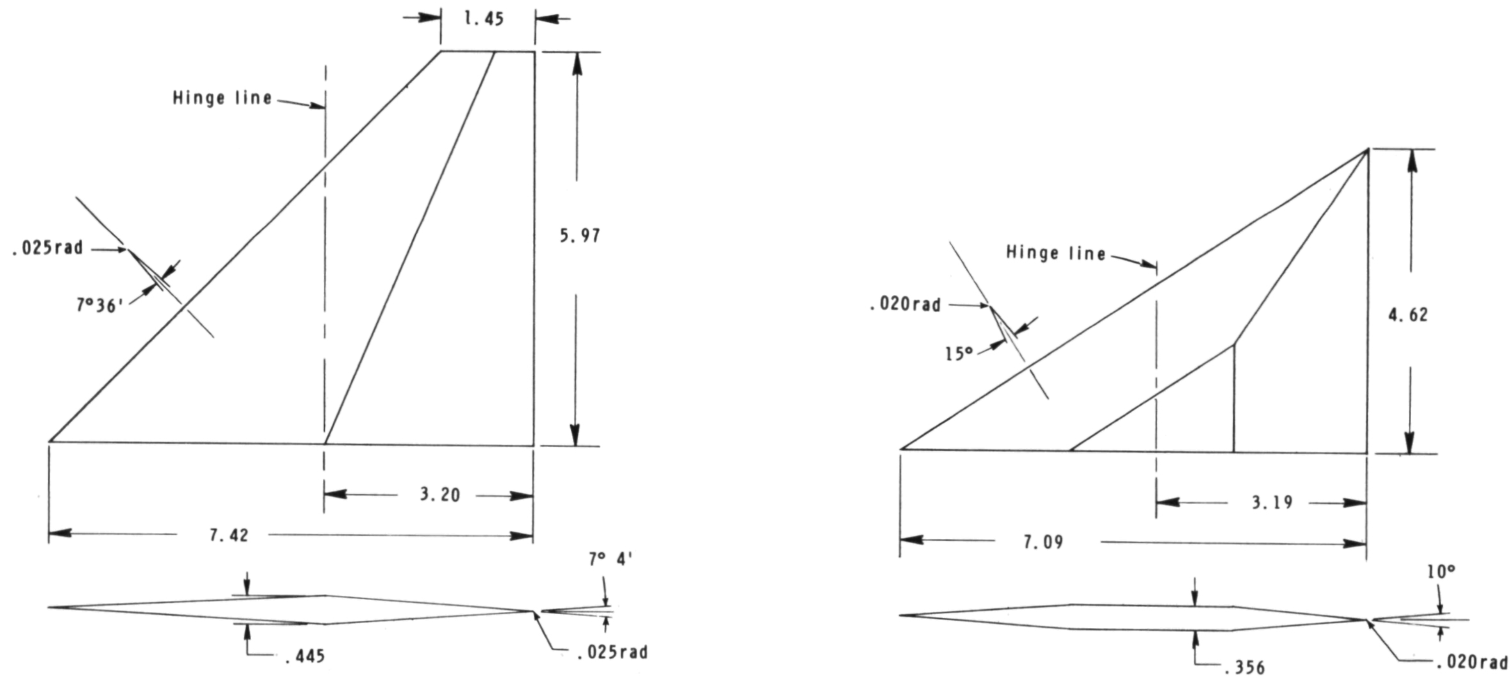

(b) Wing and tail.

Figure 3.- Concluded.

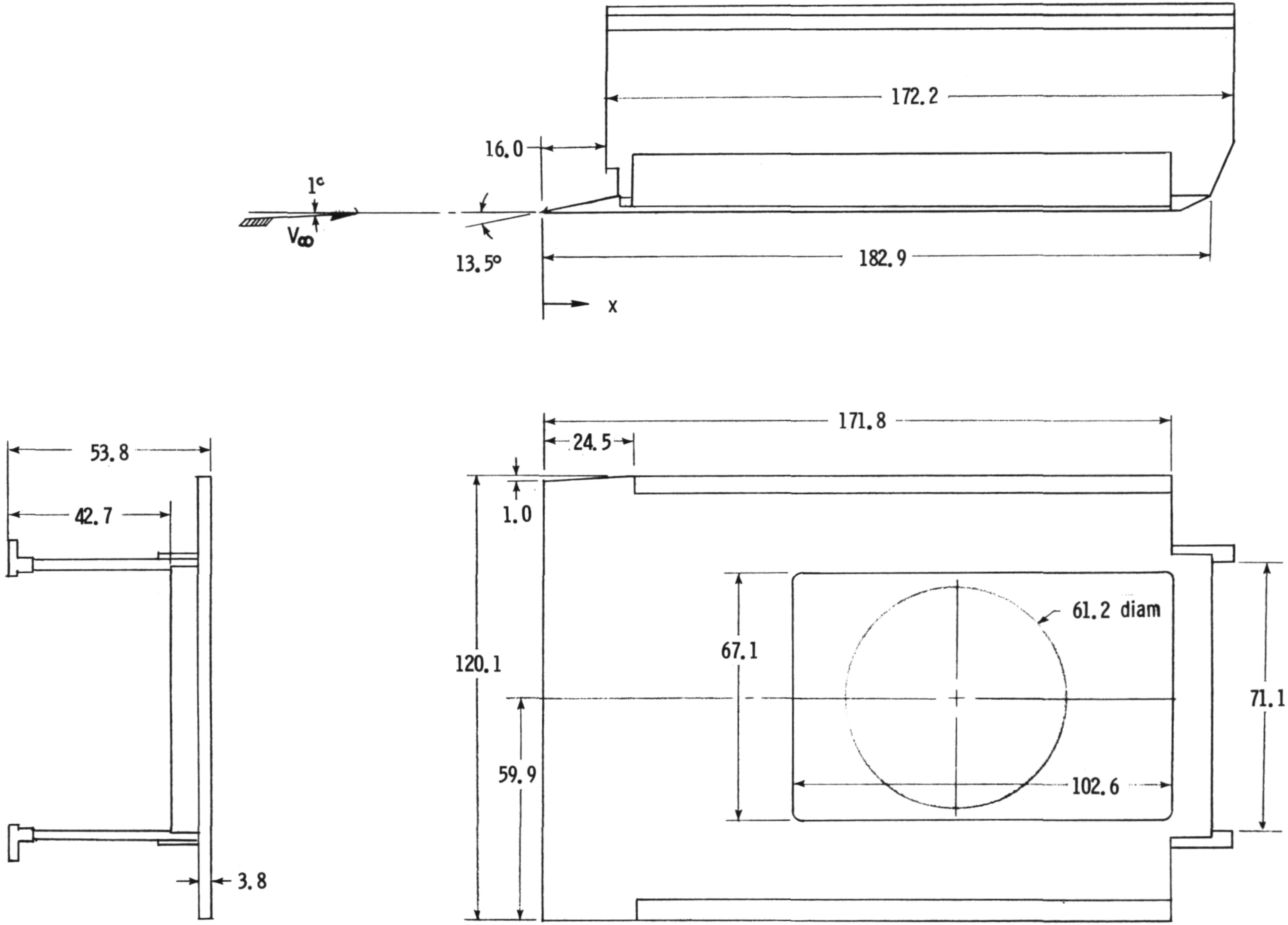

(a) Splitter-plate assembly.

Figure 4.- Splitter-plate drawings and basic dimensions. (All dimensions are in centimeters unless otherwise noted.)

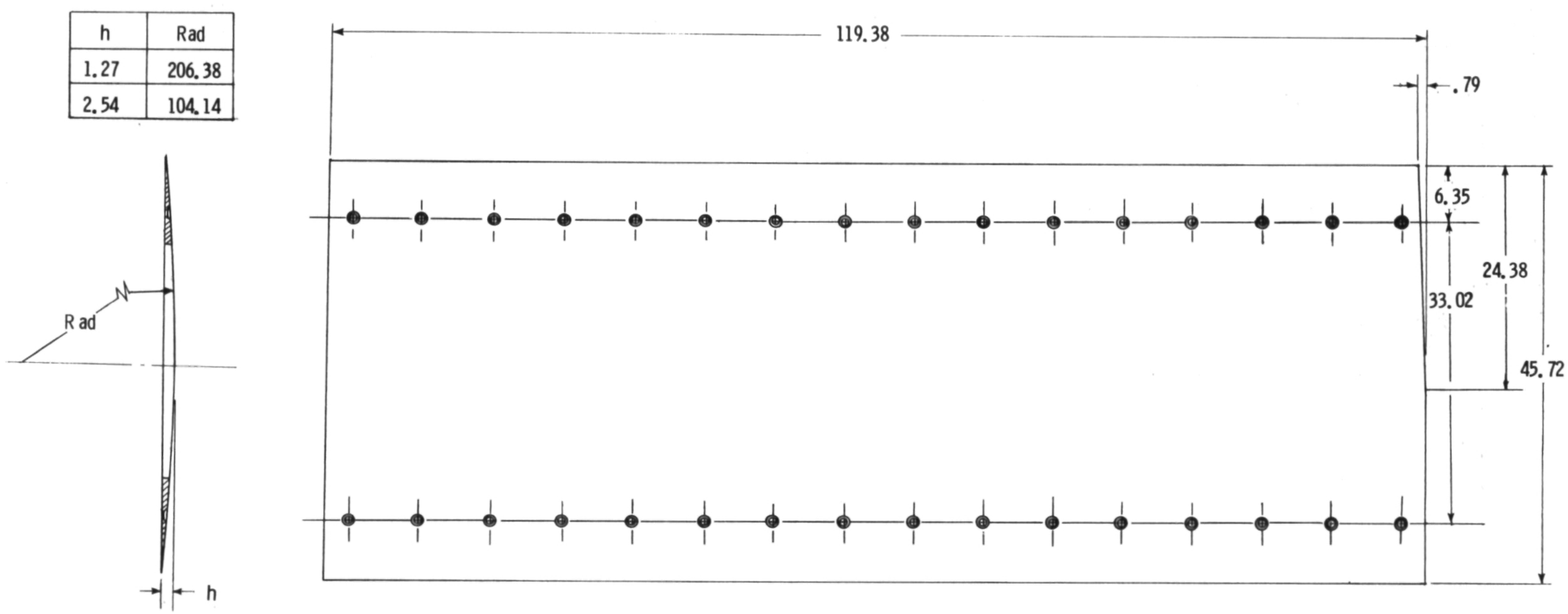

(b) Circular-arc protuberances.

Figure 4.- Concluded.

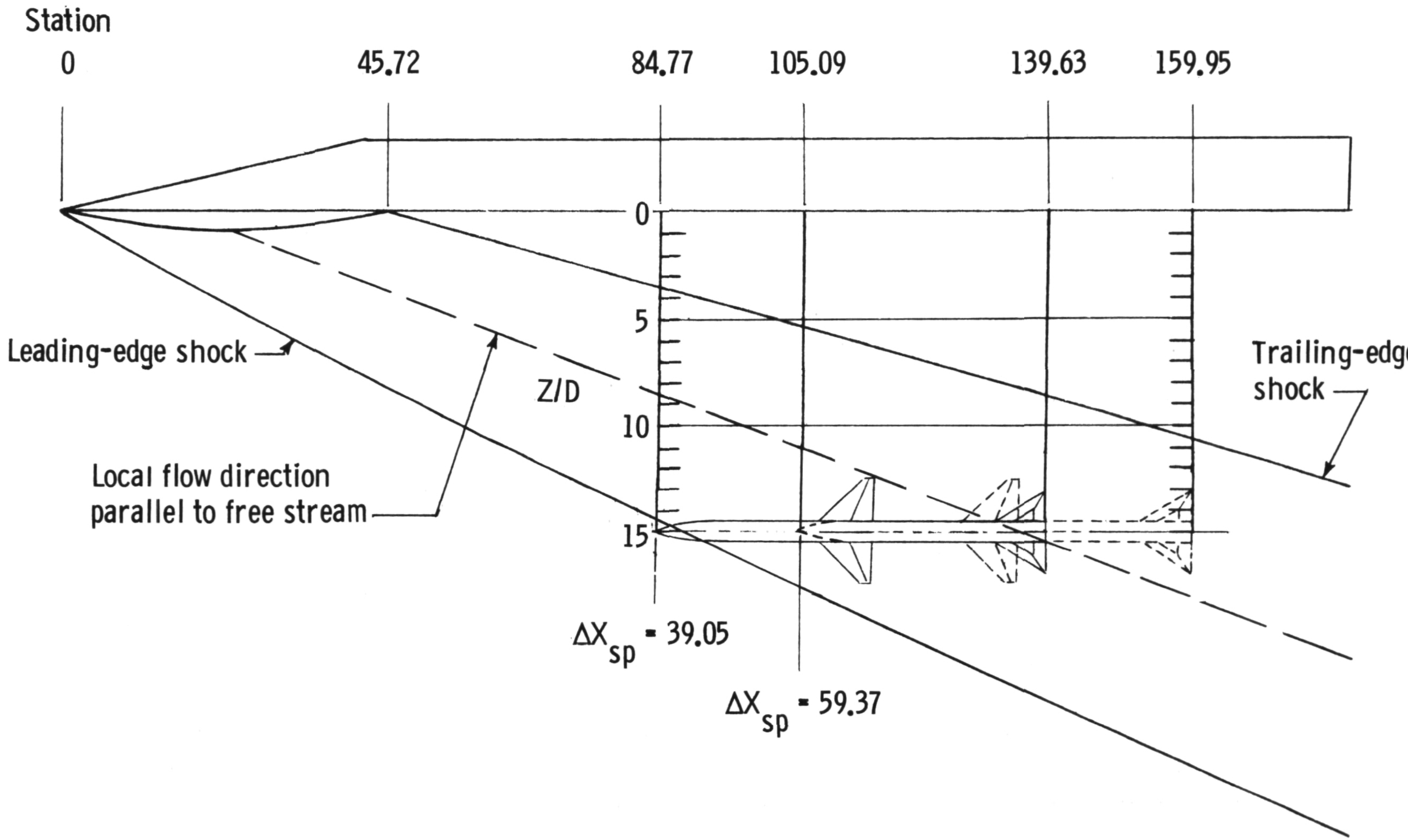

(a) $X_p = 0$; h = 1.27 cm.

Figure 5.- Store model locations relative to calculated protuberance flow field. Test range of Z/D is from 3.3 to 13.3. (All dimensions are in centimeters unless otherwise noted.)

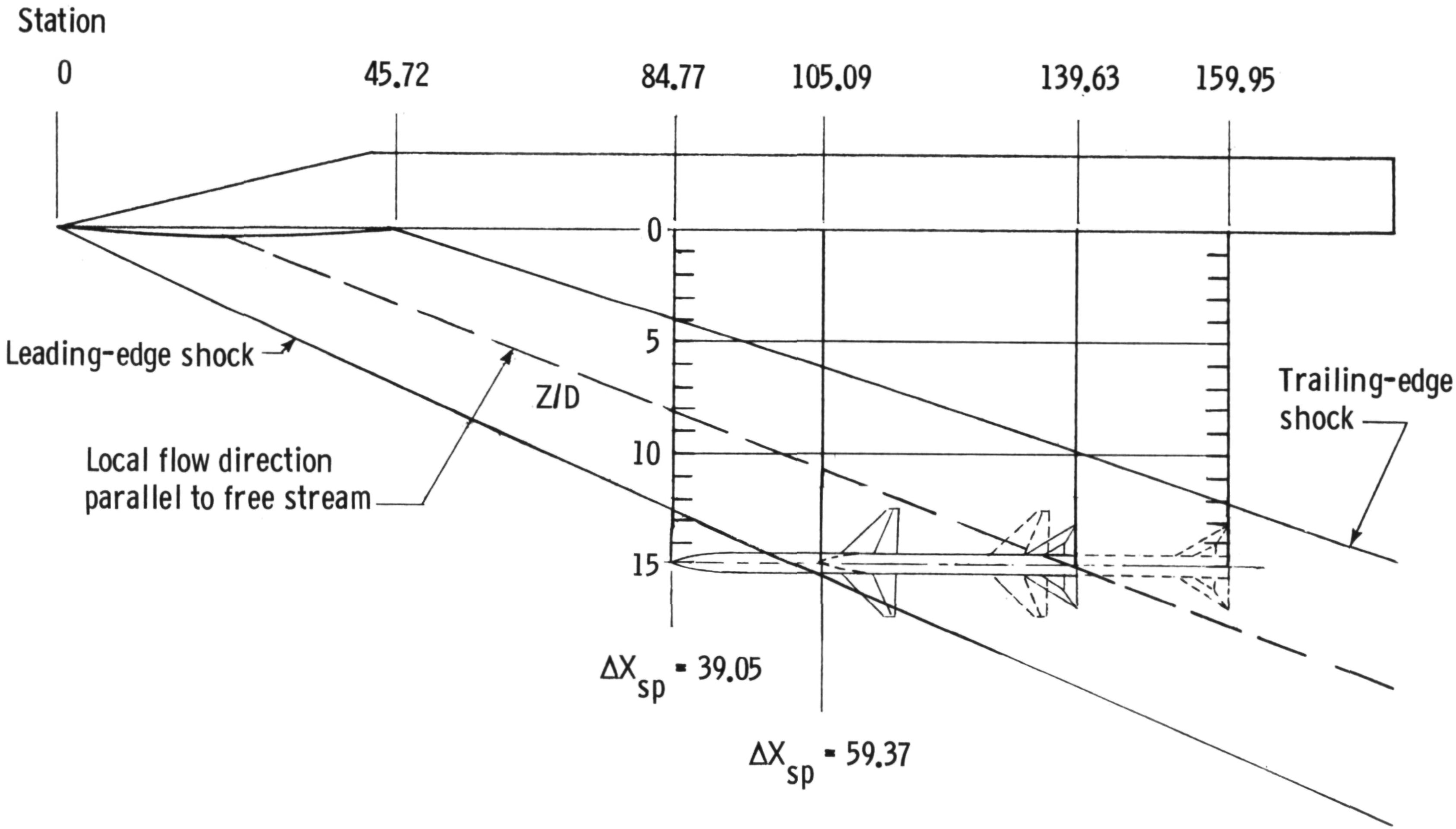

(b) $X_p = 0$; h = 2.54 cm.

Figure 5.- Continued.

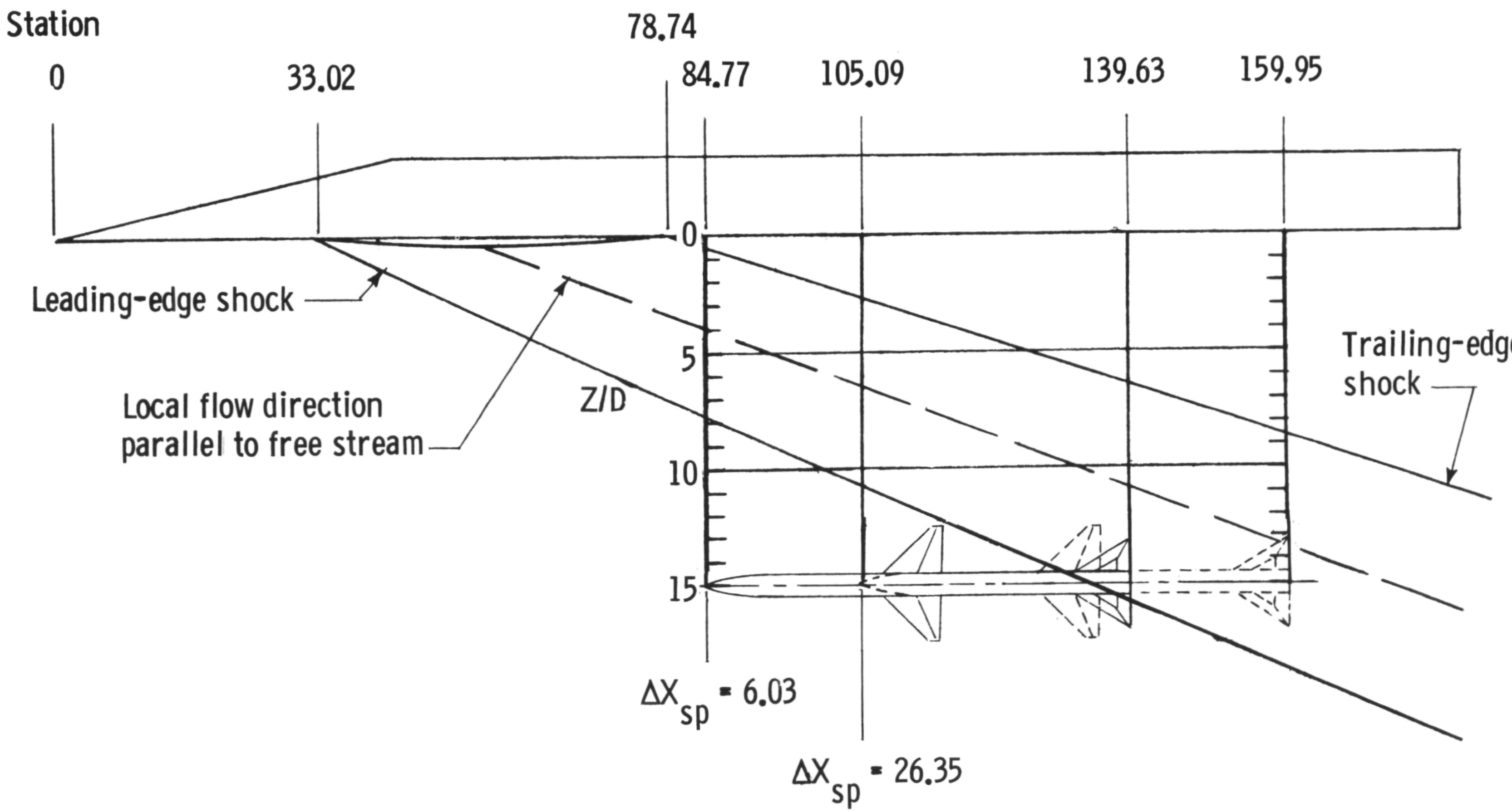

(c) X_p = 33.02 cm; h = 1.27 cm.

Figure 5.- Continued.

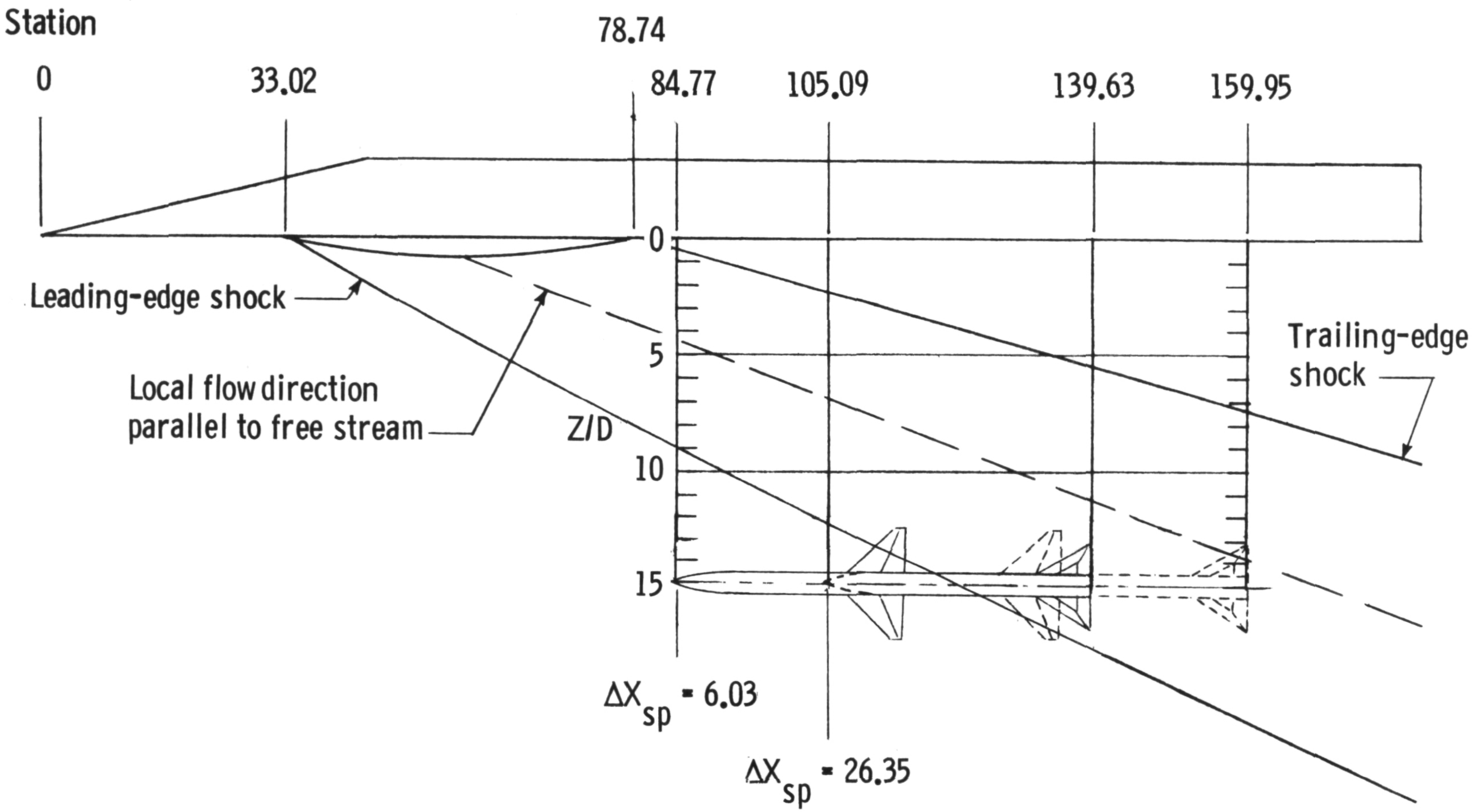

(d) X_p = 33.02 cm; h = 2.54 cm.

Figure 5.- Concluded.

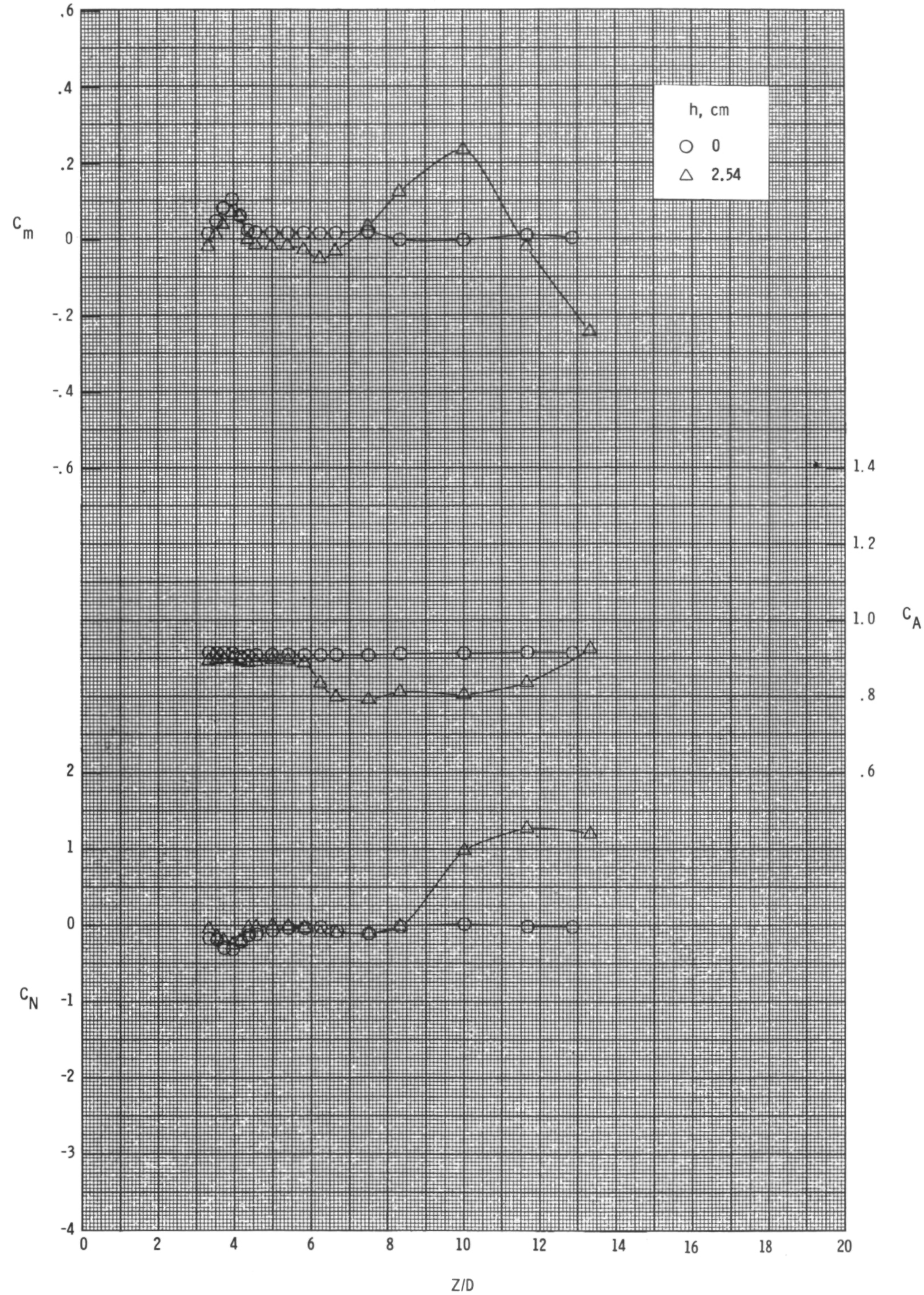

(a) $X_p = 0$; $\Delta X_{sp} = 59.37$ cm.

Figure 6.- Effect of protuberance height on store separation characteristics. $\phi = 0°$.

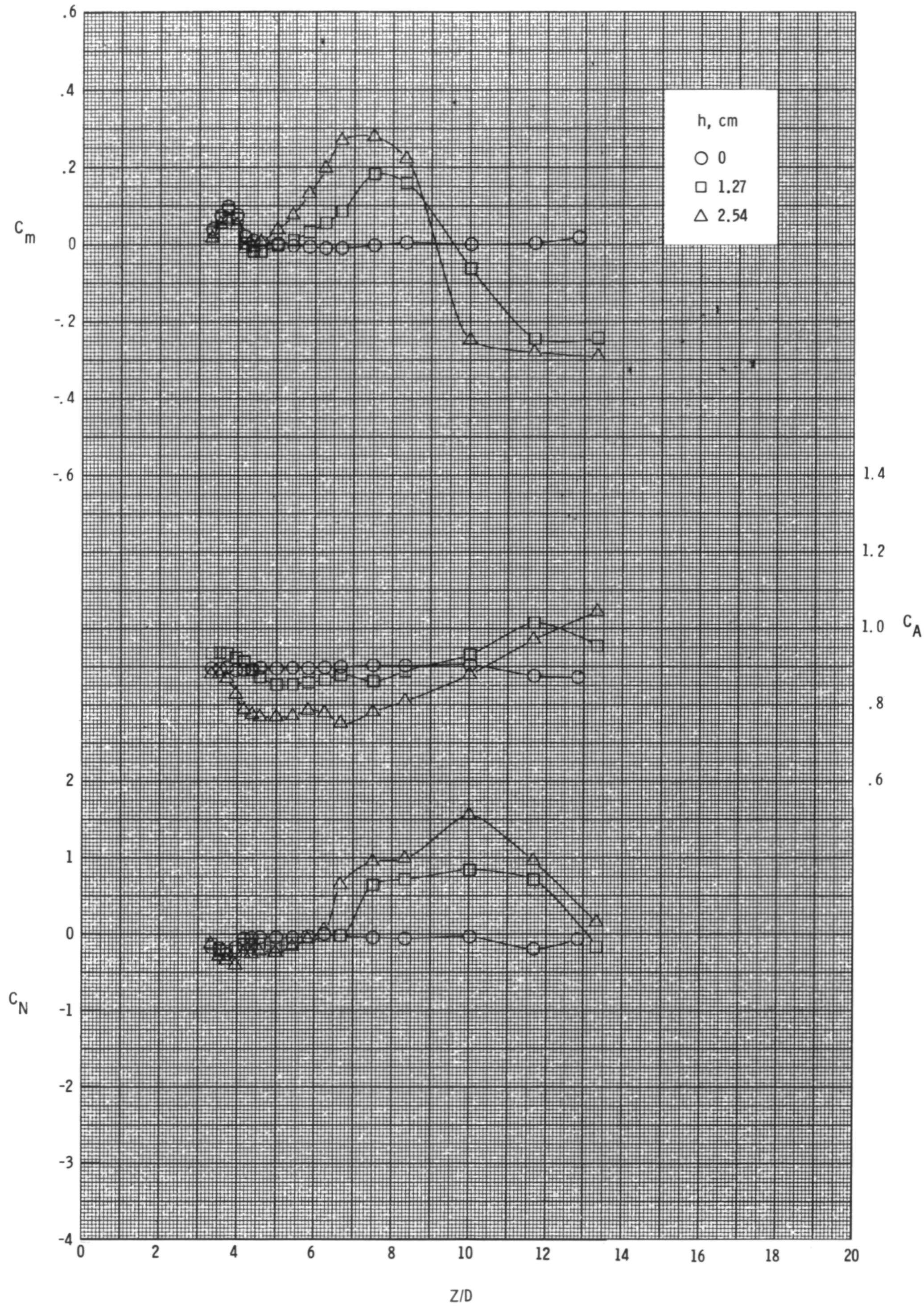

(b) $X_p = 0$; $\Delta X_{sp} = 39.05$ cm.

Figure 6.- Continued.

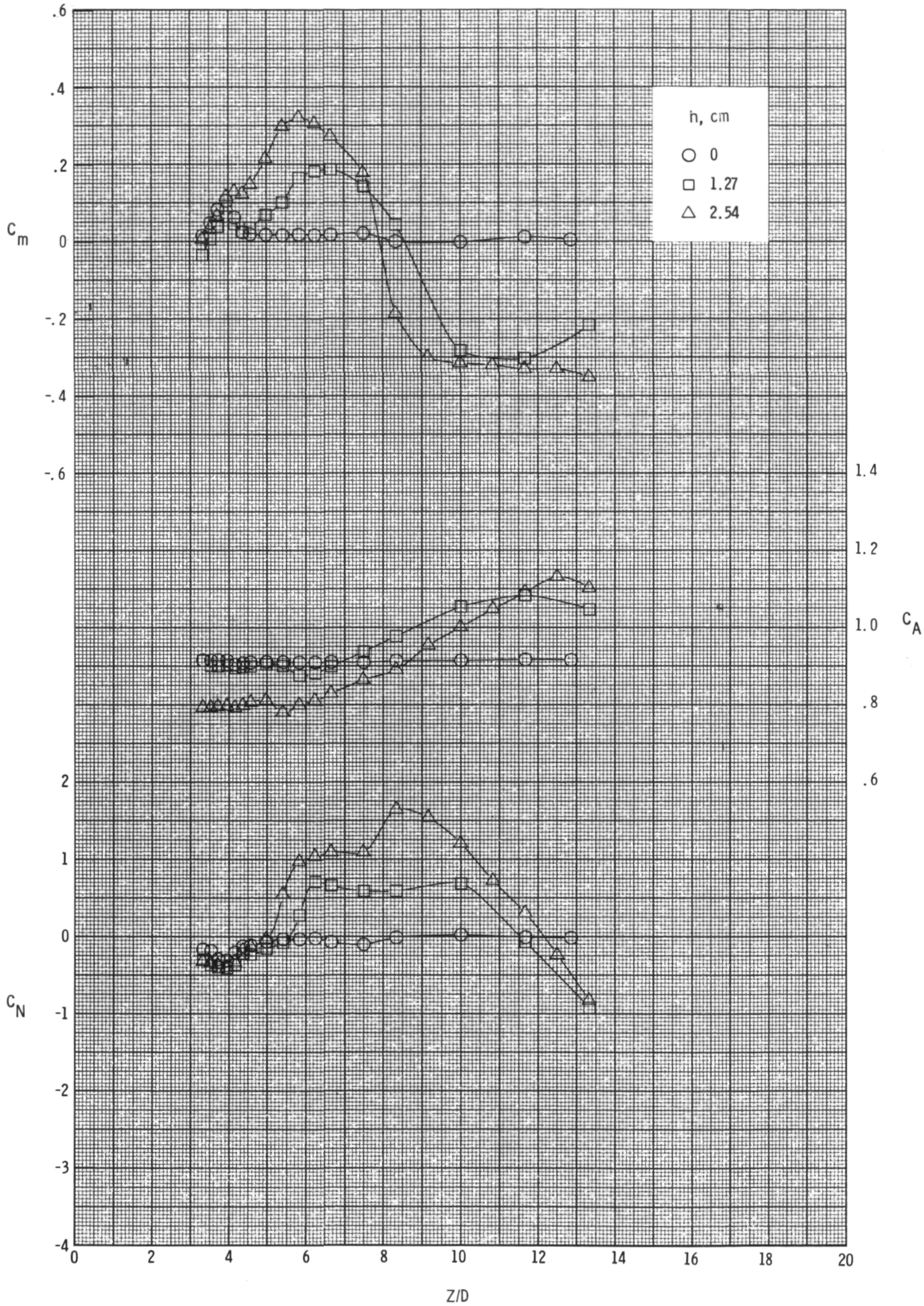

(c) $X_p = 33.02$ cm; $\Delta X_{sp} = 26.35$ cm.

Figure 6.- Continued.

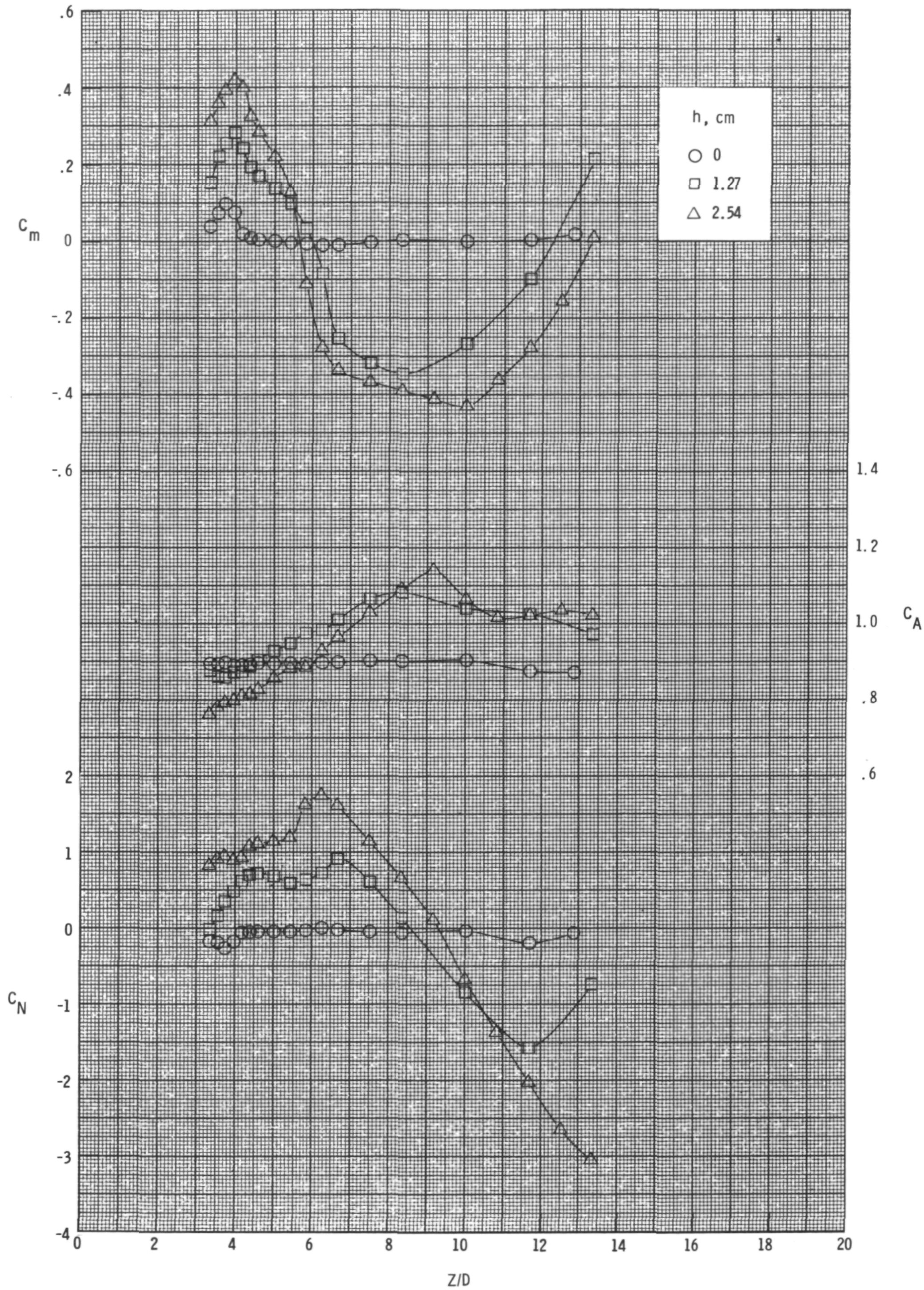

(d) X_p = 33.02 cm; ΔX_{sp} = 6.03 cm.

Figure 6.- Concluded.

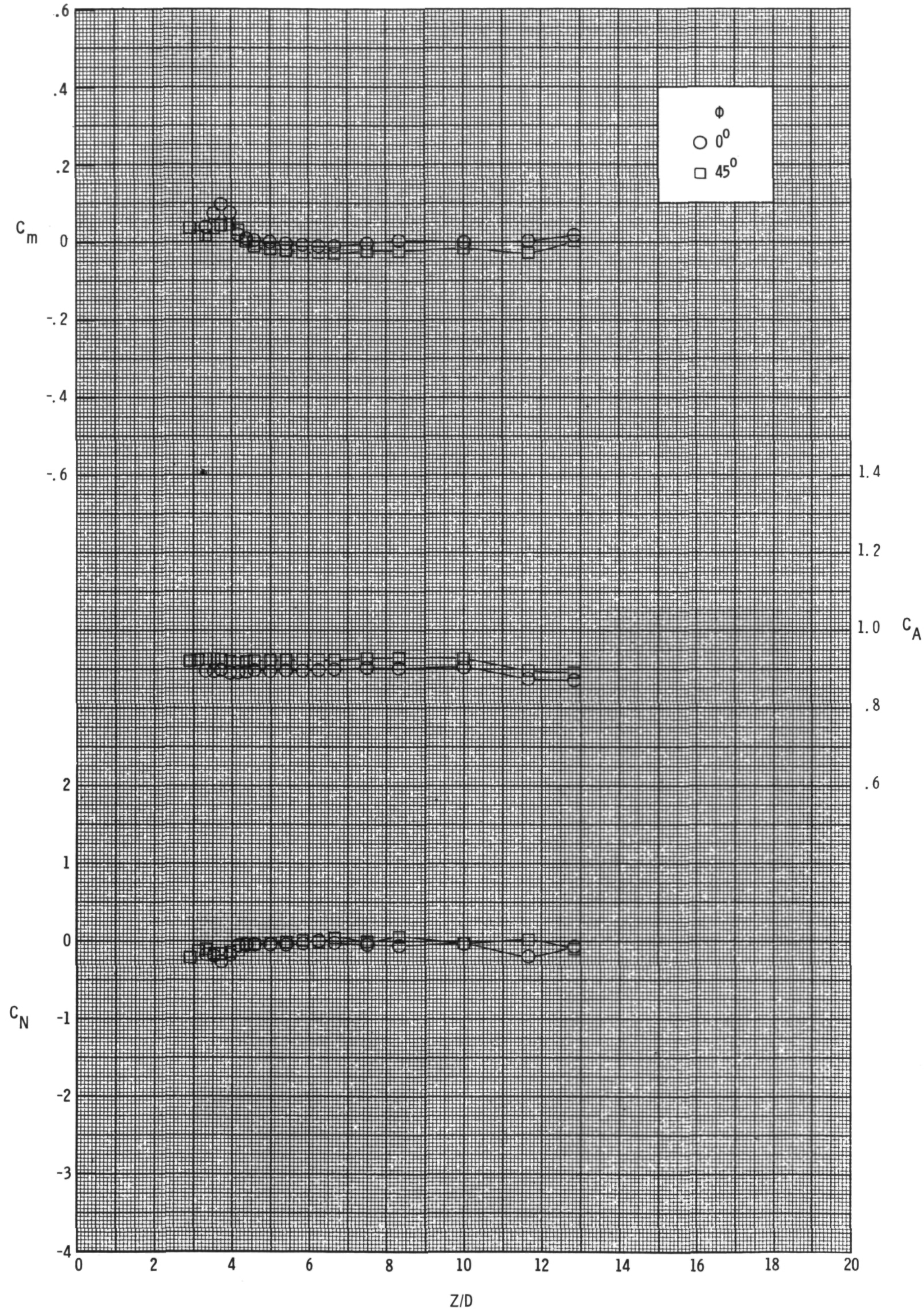

(a) h = 0; X_s = 84.77 cm.

Figure 7.- Effect of roll angle on store separation characteristics.

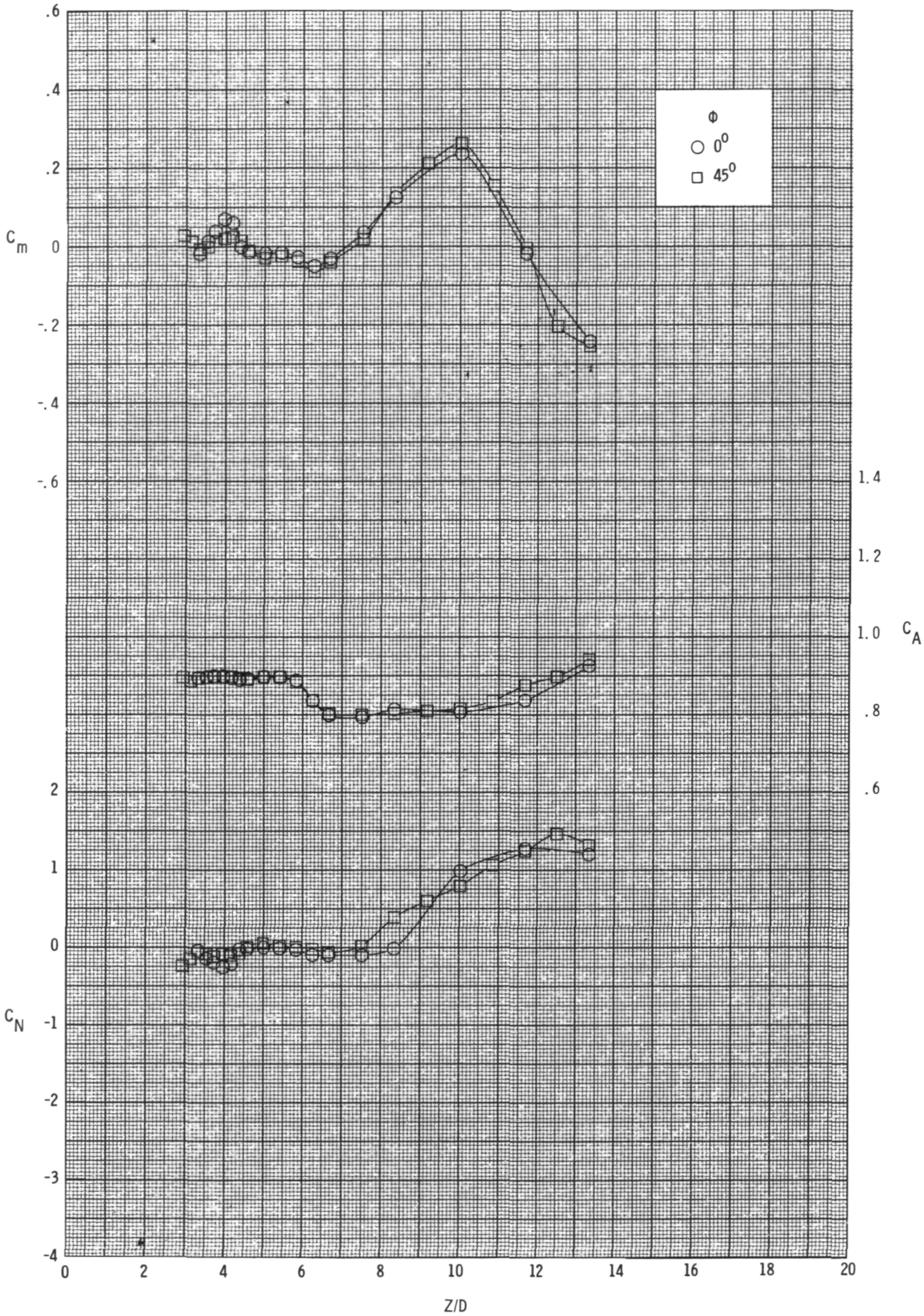

(b) h = 2.54 cm; ΔX_{sp} = 59.37 cm.

Figure 7.- Continued.

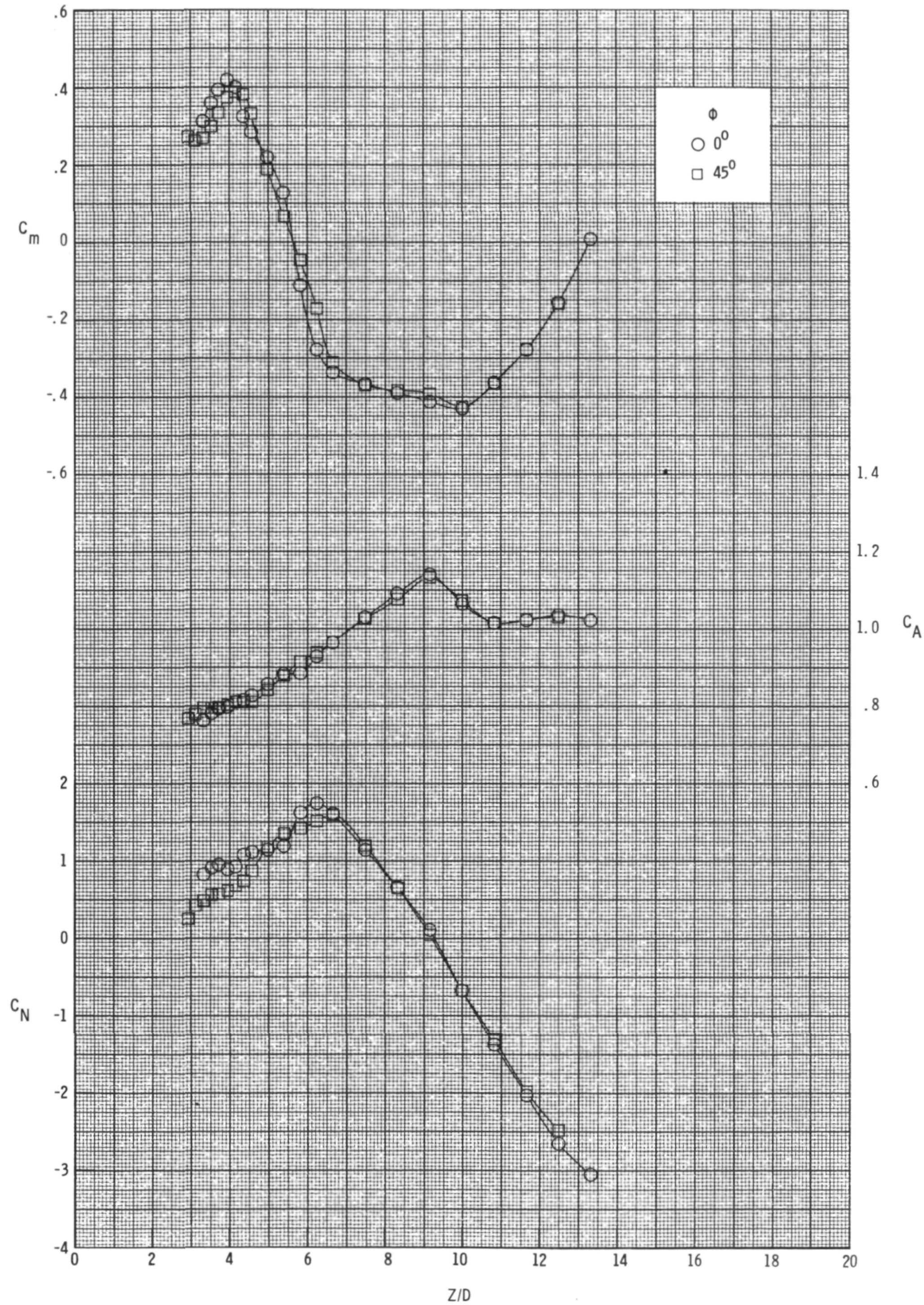

(c) h = 2.54 cm; ΔX_{sp} = 6.03 cm.

Figure 7.- Concluded.

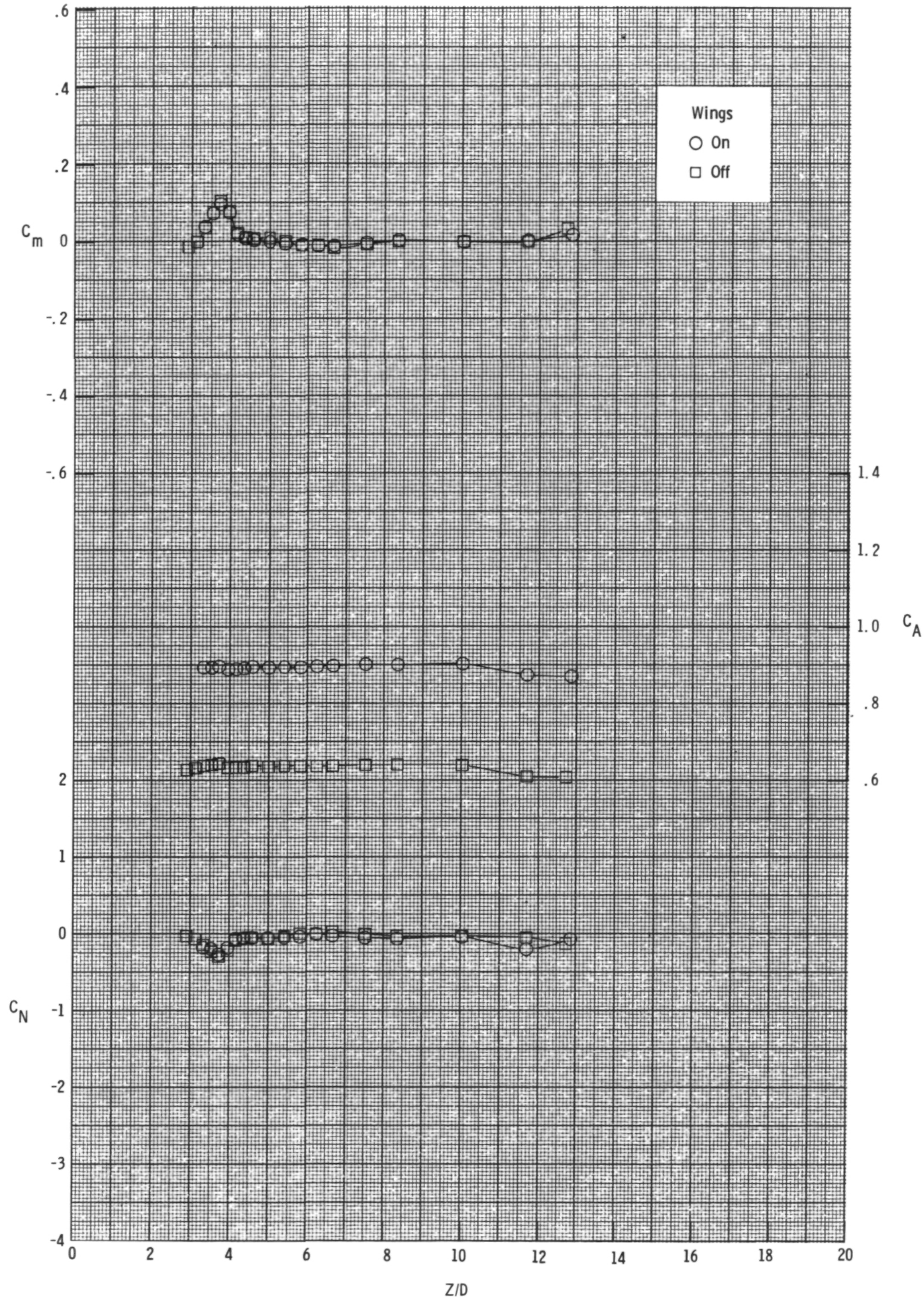

(a) $h = 0$; $X_s = 84.77$ cm.

Figure 8.- Store separation characteristics with and without wings. $\phi = 0°$.

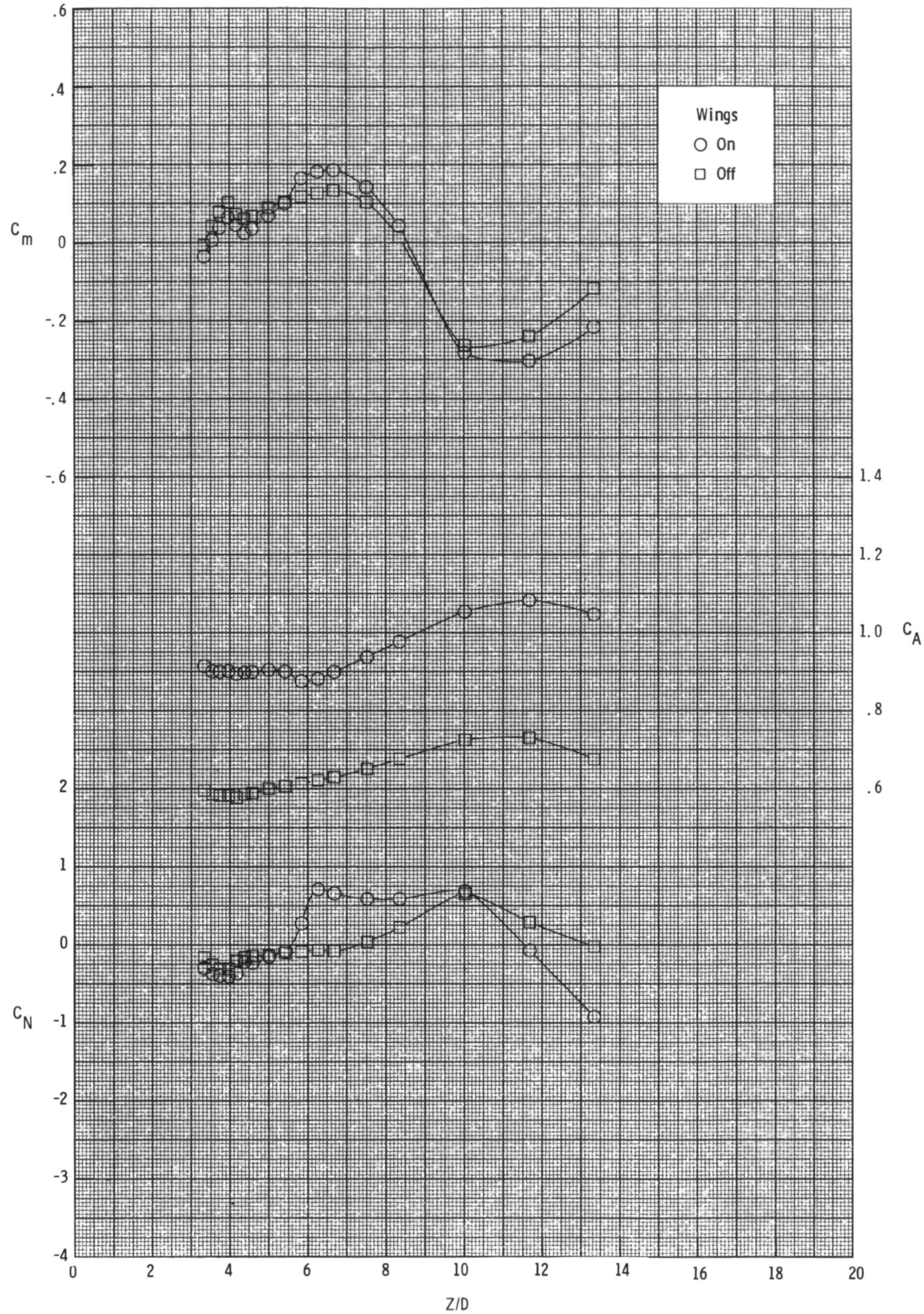

(b) $h = 1.27$ cm; $\Delta X_{sp} = 26.35$ cm.

Figure 8.- Continued.

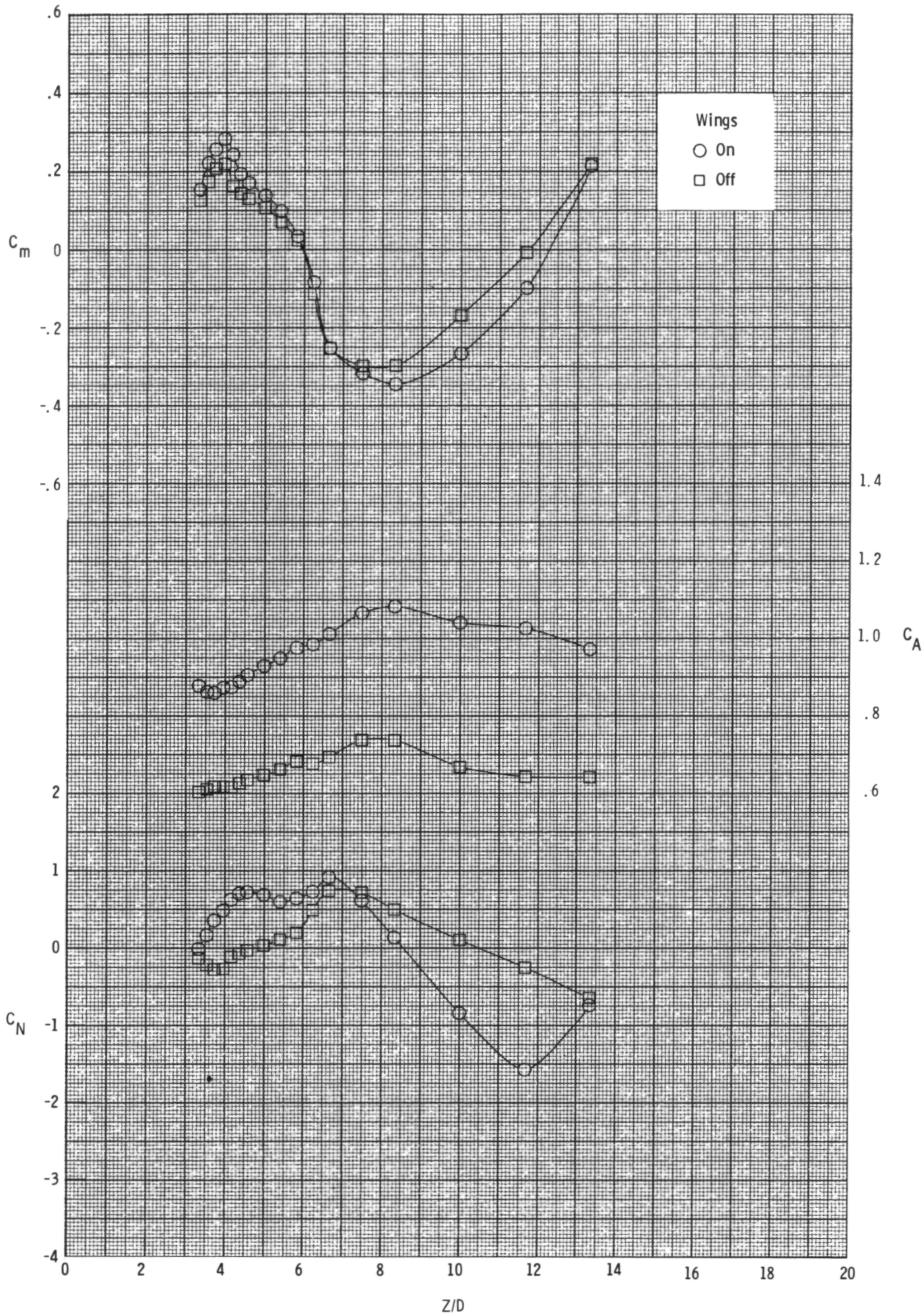

(c) h = 1.27 cm; ΔX_{sp} = 6.03 cm.

Figure 8.- Concluded.

1. Report No.	2. Government Accession No.	3. Recipient's Catalog No.
NASA TM-85713		

4. Title and Subtitle	5. Report Date
AERODYNAMIC CHARACTERISTICS OF A SPARROW III MISSILE MODEL IN THE FLOW FIELD OF A GENERALIZED PARENT BODY AT MACH 2.86	February 1984
	6. Performing Organization Code 505-43-23-02
7. Author(s) Robert L. Stallings, Jr.	8. Performing Organization Report No. L-15705
9. Performing Organization Name and Address NASA Langley Research Center Hampton, VA 23665	10. Work Unit No.
	11. Contract or Grant No.
12. Sponsoring Agency Name and Address National Aeronautics and Space Administration Washington, DC 20546	13. Type of Report and Period Covered Technical Memorandum
	14. Sponsoring Agency Code

15. Supplementary Notes

16. Abstract

Longitudinal aerodynamic characteristics of a Sparrow III wing-control missile model were measured through a range of separation distances relative to a flat-plate surface that represented the parent-body configuration. Measurements were obtained with and without two-dimensional circular-arc protuberances attached to the flat-plate surface. The tests were conducted at a Mach number of 2.86 and a Reynolds number per meter of 6.56×10^6. The behavior of these longitudinal characteristics with varying separation distance in the flow field created by the flat plate and protuberance was generally as would be expected on the basis of flow-field boundaries determined from the second-order approximation of Friedrich. In general, varying roll angle from 0° to 45° caused no significant effect on the store separation characteristics.

17. Key Words (Suggested by Author(s))	18. Distribution Statement
Store separation Aerodynamic characteristics Supersonic	Unclassified - Unlimited Subject Category 02

19. Security Classif. (of this report)	20. Security Classif. (of this page)	21. No. of Pages	22. Price
Unclassified	Unclassified	27	A03